Chemically-Addressable Protein Entrapment in Silica Sol-Gels

Wenlan Yang

A thesis

submitted in partial fulfillment of the

requirements for the degree of

Master of Science

University of Washington

2016

Committee:

François Baneyx, Chairman

Qiuming Yu

Program Authorized to Offer Degree:

Chemical Engineering

University of Washington

Abstract

Chemically-Addressable Protein Entrapment in Silica Sol-Gels

Wenlan Yang

Chair of the Supervisory Committee:

François Baneyx, Chairman

Department of Chemical Engineering

Silica-based sol-gel materials as carriers for immobilization of biological species and subsequent controllable release have experienced great examination since past decade. The transparent and robust network possesses inert and stable physicochemical properties, allowing a variety of biomolecules to be successfully entrapped, including proteins, antibodies and antigens, cells. Controlled and effective release is usually achieved by functionalization of the silica matrices to physically cap the pores by modified nanoparticles serving as nanovalves. In this study, fusion proteins with a designed silica-binding peptide tag are immobilized during the sol-gel formation, and subsequently be released with a tag-specified eluent. The release kinetics have

been studied under various conditions to demonstrate the chemically-addressable tag-mediated protein sequestration in silica sol-gel matrices.

Acknowledgements

I would first like to thank my primary investigator professor François Baneyx for the continuous support of my master study and research, for his great enthusiasm and immense knowledge.

Besides my advisor, I would like to thank Dr. Qiuming Yu in my thesis committee for her encouragement and enlightenment.

My sincere thanks goes to Brittney Hellner for assistance during my thesis project. I thank my fellow labmates in Baneyx Group: Kannan Aravagiri, Dr. Brandon Coyle, Sonja Glaser, Chia-Wei Hsu, Dr. James Matthaei, Dr. Brian Swift, Jessica Soto-Rodríguez, Alexander Thomas and Dr. Weiran Zhang. My thanks also goes to Jared Shadish in DeForest Lab, Chad Curtis in Nance Lab, and Matthew Lim in Pauzauskie Lab.

Introduction

The entrapment of biological species within mesoporous materials has been widely investigated in drug delivery since 2001 when Ibuprofen® was first successfully delivered from mesoporous nanoparticle MCM-41.[1] Among accessible nanomaterials, silica-based systems have been extensively studied mainly due to the tunable physicochemical characteristics and stimuli-responsive properties.[2, 3] Typically, the sol-gel derived materials allow formation of transparent wet gel at room temperature with encapsulation of biological species in a functional state. It is chemically-inert, mechanically-stable with negligible swelling.[4] The network possesses high surface area and volume capacity, less shrinkage, and the ability to obtain desired shape and form. With a broad distribution in pore size ranging from 2 nm to 40 nm, a variety of biomolecules can be entrapped, such as enzymes, antibodies, and cells.[5] Basically, there are two ways to immobilize biomolecules in sol-gels. The first approach is to form the sol-gel network in the presence of the biomolecules. The alternative way is to load the molecules afterwards. Both methods have advantages. For example, the prior method provides tighter confinement which cannot be easily achieved by simple adsorption happened in the second method. While the later approach can avoid possible adverse effect on the biomolecules entrapped during the sol-gel formation.[6] Current sol-gel encapsulation applications have been focused on areas such as therapy, diagnostics, drug production and tissue engineering.[7, 8]

With achievement of entrapping biomolecules, studies have been moved to long-term storage and controlled release of the active biological species. Although the release could be controlled by the size of the pores partly, “zero premature release” before reaching targeted cells or locations is highly favorable in effective drug delivery systems.[9] Two main strategies are commonly applied: covalent and cleavable bonds between the targeted molecules and the support;

functionalized coatings on the surface that can be modified upon environmental changes.[10] Work from Lai and coworkers serve as an example as the prior approach, which shows controlled release with the aid of CdS nanoparticles capping on the silica surface by cleavable disulfide bonds.[11] The blocking prevents untimely release and can be removed upon specific chemical stimulations. The later approach is widely demonstrated by nanovalves using tunable conditions such as pH, redox, and enzymes as actuators.[12]

A previously designed dodecapeptide Car9 shows micromolar affinity for silica through electrostatic interactions between negatively-charged silanol groups and basic residues.[13, 14] These interactions can be interrupted by Arginine, introducing the possibility of fast and inexpensive protein purification[13] and chemically tunable microcontact printing of proteins.[15] This discovery has drawn us to study the chemically-addressable protein entrapment in silica sol-gel matrices and subsequent controlled release for potential applications, particularly with drug delivery. We proposed that Car9-tagged fluorescent protein can be entrapped in silica matrices during sol-gel polymerization process and subsequently be released via Arginine supplementation. The controlled release of sol-gel bound Car9-tagged fluorescent protein was experimentally determined through time-dependent measurement of the supernatant fluorescence, and examined qualitatively by UV and confocal microscopies. The controlled release was further investigated under various conditions, such as the size of the silica particles, pH of the elution buffer, stability against thermal effects, discontinuous release, multiple tagged-protein release, and compared to a series of control experiments. This study takes a closer look at the behavior of Car9-tagged fluorescent protein bound to silica sol-gel matrices, and the controlled release is further generalized to serve as a model for efficient drug delivery systems.

Results and Discussion

Entrapment of Car9-tagged proteins within hemispheroidal silica sol-gels. Kröger and coworkers previously described R5, a peptide of amino acid sequence SSKKSGSYSGSKGSKRRIL that constitutes a repeating unit of the silica-precipitating (and heavily post-translationally modified) silaffin protein from the diatom *Cylindrotheca fusiformis*.[16] In a synthetic form, and at a concentration of 10 mg/mL, R5 catalyzes the precipitation of silica from silicic acid solutions within seconds.[16, 17] This property that has been exploited to sequester functional enzymes within the precipitated phase.[18]

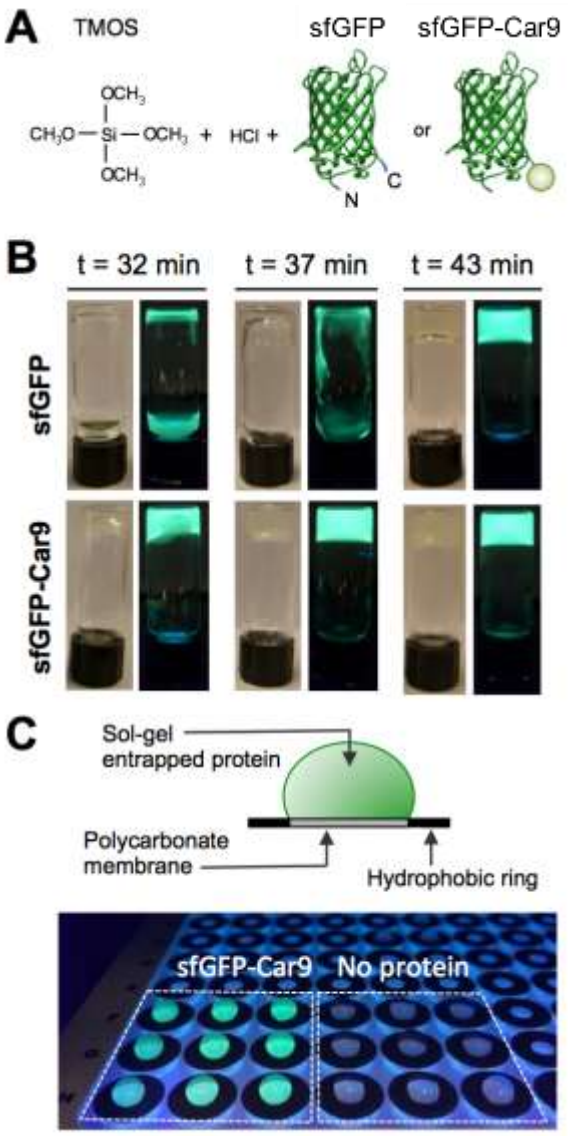

Figure 1. Entrapment of sfGFP and sfGFP-Car9 within silica sol-gels. (A) Schematic illustration of the process and proteins. (B) The ability of sfGFP and sfGFP-Car9 (10 μM) to drive sol-gel formation was compared by inversion experiments at the indicated time points. Vials were photographed under ambient and UV light. (C) Formation of hemispheroidal sol-gel particles on ChemoTx® plates.

Here, we sought to determine if a fused Car9 tag would similarly support the entrapment of proteins to which it is fused. To test this possibility, we pre-hydrolyzed a solution of tetramethoxysilane (TMOS) essentially as described[18] and supplied the resulting silicic acid solution with 10 μM (~ 0.3 mg/mL) of superfolder green fluorescent protein (sfGFP)[19] or with the same concentration of sfGFP-Car9, a sfGFP

variant fitted with a C-terminal Car9 tag via a KLGGGS linker (Figure 1A).[15] Under our experimental conditions, we did not observe any silica precipitation, presumably because we used the proteins at a 500-fold lower molarity than the R5 peptide concentration employed by Luckarift et al.[18] However, both solutions gelled into fluorescent monoliths after about 30 min (sfGFP-Car9) or 40 min (sfGFP) incubation at room temperature (Figure 1B). The ~30% faster rate of sol-gel formation observed with sfGFP-Car9 was entirely due to the Car9 extension since we found no difference in gelation times between sfGFP and sfGFP-CT43, a fusion protein between sfGFP and CT43, a dodecameric peptide that binds to zinc sulfide[21] (Figure S1 in Supporting Information). We conclude that while Car9-tagged proteins do not precipitate silica from silicic acid at micromolar concentrations, the Car9 tag catalyzes the condensation of the precursor into a sol-gel network.

To more conveniently handle protein-loaded sol-gels, we produced hemispheroidal particles by depositing 30 µL of protein-silicic acid solution onto circular polycarbonate membranes bounded by hydrophobic rings using the ChemoTx® system (Figure 1C). After 4h incubation in sealed chambers to ensure complete polymerization, particles were transferred to Tris-HCl buffer for characterization of protein release kinetics.

Chemical control of Car9-tagged protein release. The equilibrium dissociation constant (K_d) between Car9-tagged proteins and silica surfaces is 1 µM.[13] Although the interaction is not affected by high salt concentrations (5M NaCl or $MgCl_2$), it is competitively disrupted in the presence of 1M Arginine.[13, 15] (Lysine solutions can be used for the same purpose but we did not use this amino acid because it fluoresces in the GFP excitation window.) To determine how Car9 tagging would affect protein release from sol-gels, we placed single hemispheroidal particles in Tris-HCl solutions buffered at pH 7.5 or 8.5 and quantified the

amount of fluorescence released in the supernatant as described in the Experimental Section. In the absence of additive and at a pH of 7.5, about 7% of the encapsulated sfGFP was released after 6h (assuming 100% entrapment and no protein denaturation during particle formation). This value rose to 17% after 24h (Figure 2A, open squares) and to 22% after 48h. Under the same conditions, no sfGFP-Car9 made its way into the supernatant as fluorescence remained at background levels (Figure 2A, open circles). Inclusion of 1M Arginine in the buffer triggered sfGFP-Car9 release and facilitated the spontaneous elution of sfGFP (Figure 2A, closed symbols).

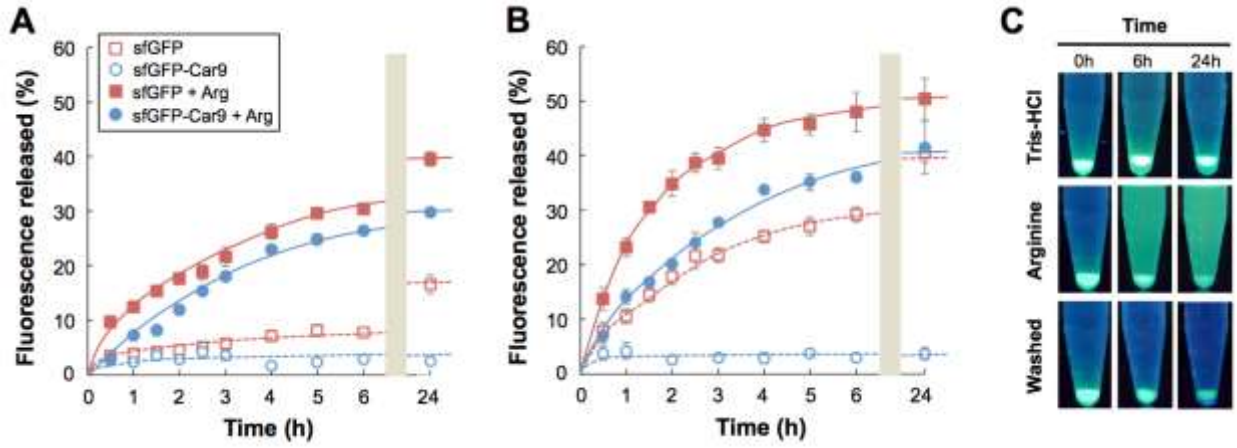

Figure 2. Effect of pH and Arginine on the release of sfGFP and sfGFP-Car9 from hemispheroidal sol-gel particles. sfGFP or sfGFP-Car9 (10 µM) entrapped in hemispheroidal silica particles were incubated at room temperature with shaking in 1 mL of 20 mM Tris-HCl buffered at pH 7.5 (A) or 8.5 (B) and containing or lacking 1M Arginine (Arg). The fluorescence released in the supernatants was assayed at the indicated time points. Error bars correspond to triplicate independent experiments. A value of 100% corresponds to the fluorescence of a 10 µM solution of sfGFP or sfGFP-Car9. (C) Appearance of particles and supernatants under UV illumination at 365 nm following 0, 6 and 24h incubation in Tris-HCl or Arginine-containing solutions. The lower panel shows the appearance of Arginine-treated particles following removal of the supernatant and buffer wash.

A pH of 8.5, which should partially decrease the charge of the Car9 extension (pI = 11.1), magnified these differences (Figure 2B-C). Whereas sfGFP-Car9 remained quantitatively retained within particles incubated in Arginine-free buffer, sfGFP leached into the solvent at a

10-fold higher initial rate than at pH 7.5 and twice more protein had reached the supernatant at the 24h time point (Figure 2B-C, open squares; Figure S2). As expected, inclusion of Arginine in the buffer further promoted sfGFP leaching and triggered sfGFP-Car9 release (Fig. 2B). About 42% of the entrapped Car9 fusion protein reached the supernatant after 24h of incubation (compared to 50% for sfGFP) and there was no further release of either protein when incubation was pursued for an additional 24h. Based on the fact that particles remain fluorescent after 24h of Arginine treatment (Figure 2C), and assuming that no denaturation takes place during sol-gel formation, we estimate that ~50% of the entrapped proteins remains confined within hemispheroidal sol-gel particles or are released with much more slowly than the timescale considered in this study. Why sfGFP-Car9 is released by Arginine with twofold slower initial kinetics relative to unmodified sfGFP is likely due to Car9-mediated cycles of binding and release to the silica matrices. Subtle differences in pore structure associated with a faster silicic acid condensation rate (Fig. 1B) may also contribute to the observed differences.

To summarize, the Car9 tag catalyzes silica sol-gel formation and confines proteins to which it is fused to the inorganic matrices. Protein release is entirely dependent on the presence of a Car9-specific eluent such as Arginine and the kinetics and extent of release can be tuned by manipulating the solution pH to modulate the biotic-abiotic interaction.

Entrapment of Car9-tagged proteins within spherical silica sol-gels. To more easily entrap Car9 fusion proteins within silica sol-gels and further characterize Arginine-induced protein release, we developed a process in which a mixture of silicic acid and sfGFP-Car9 is injected into silicone oil to produce protein-loaded spherical particles of tunable sizes (Fig. 3A). SEM imaging showed that the sol-gels thus produced consist of a connected network of fused silica spheres in the 50-100 nm diameter range (Figure 3B). While nanosphere packing was

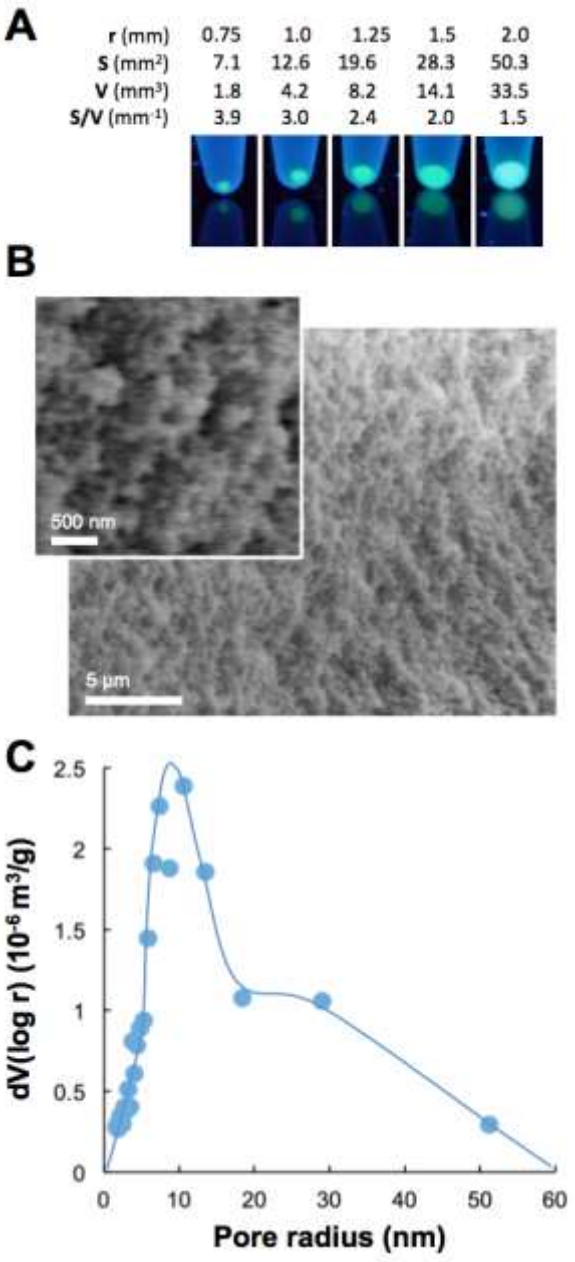

Figure 3. Synthesis and characterization of spheroidal particles produced in the presence sfGFP-Car9. (A) Appearance of particles of various sizes under UV illumination. (B) SEM images of fractured particles at two magnifications. (C) Pore size distribution determined by BJH analysis of particles subjected to supercritical drying.

generally tight, larger voids were not uncommon (Figure 3B, inset). Consistent with this morphological characterization, BJH analysis revealed that although there is a clear peak corresponding to a mean pore size of ~7.5 nm, a broad distribution of larger pores is also present (Figure 3C). The surface area of particles subjected to critical point drying was ~410 m^2/g. This value is about twofold less than some of the highest surface area mesoporous silica (e.g., MCM-41). However, it is comparable to the surface area of sol-gels produced by chemical conversion of silicon alkoxides,[22-24] and over 55-fold higher that reported for bio-precipitated silica.[19] Overall, the pore size and large surface area of the spherical silica sol-gels particles produced in silicone oil appear ideal for protein entrapment.

Controlled release of Car9-tagged proteins from spherical sol-gels. Preliminary experiments revealed that when particles produced as above were washed in buffer and incubated with Arginine to liberate entrapped

sfGFP-Car9, the supernatant fluorescence stopped rising after 1h, started to decrease after 3h and reached background levels after 24h incubation. This behavior is indicative of a sfGFP-Car9 unfolding event mediated by exposure to silicone oil.[25] It was corrected by including the detergent Tween 20 in the wash buffer to remove surface-adsorbed oil and eliminate interfacial protein denaturation (Figure S3). All subsequent protein release experiments were conducted in solutions buffered at pH 8.5 to magnify differences between protein release profiles (Fig. 2).

Figure 4 shows that unlike with hemispheroidal particles solidified in air, a small amount of sfGFP-Car9 escaped the spherical particles upon incubation in buffer alone (10 or 11% of the original protein load was released after 24h, and 16 or 21% after 48h for 1 mm or 2 mm radius particles, respectively). The reasons for this discrepancy are unclear but may be related to a difference in the size of the pore mouths or to remodeling of the silica structure upon transfer of the particles to aqueous medium.

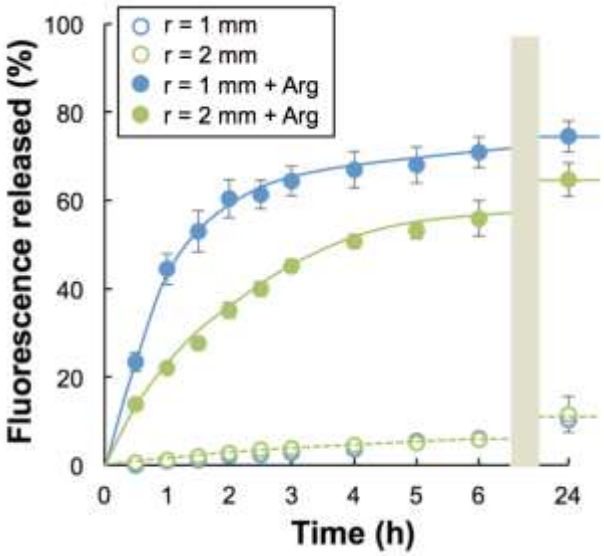

Figure 4. Influence of size on the release of sfGFP-Car9 from spherical sol-gel particles. Protein (10 μM) was entrapped within 1 or 2 mm radius particles as described in Experimental Procedures. A single 2 mm radius particle or four 1 mm radius spherical particles were transferred to 20 mM Tris-HCl, pH 8.5 buffer lacking (open symbols) or containing 1 M Arginine (closed symbols). The fluorescence in the supernatants was assayed at the indicated time points. Error bars correspond to triplicate independent experiments. A value of 100% corresponds to the fluorescence of a 10 μM solution of sfGFP-Car9.

As expected, Arginine supplementation led to efficient release of entrapped sfGFP-Car9 with initial kinetics and an extent that increased with decreasing particle size owing to an increase in surface to volume ratio (Figures 4 and 3A). Under

our experimental conditions, ~75% of the protein entrapped in 1 mm radius spheres was released after 24h incubation with Arginine. Half of this amount leached during the first 50 min and only 3% additional release was observed at 48h. For 2 mm radius spheres, 65% (respectively 68%) of the entrapped material was released within 24h (respectively 48h) and half of the protein exited the particles in ~110 min (Fig. 4, solid symbols). Fitting of the data with the Ritger-Peppas model[26] (with admittedly unmet assumptions) yielded effective diffusion coefficients ranging between 1 x 10^{-7} and 2 x 10^{-7} cm^2/s (Figure S4). These values are comparable to the range of diffusivities reported for horse radish peroxidase in silica sol-gels (0.5 x 10^{-7} to 4 x 10^{-7} cm^2/s)[27] and about 4 to 9-fold lower than the diffusion coefficient of GFP in water (8.7 x 10^{-7} cm^2/s).[28]

To gain additional information on the process of Arginine-mediated release, we used confocal fluorescence microscopy to image small and large particles at ~1/2 or 1/4 depth. Although the entire cross sections were fluorescent at initial time points, some regions were brighter than others, indicating non-homogeneous distribution of sfGFP-Car9 within the particles (Figure 5, top panels). After 6h of incubation with Arginine, most of the fluorescence was confined to the center of the cross-section as would be expected

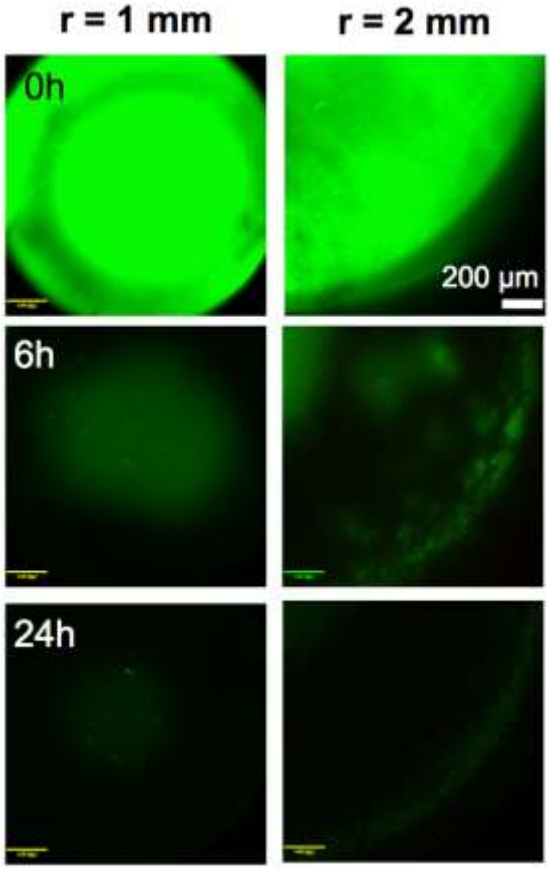

Figure 5. The cross-section of 1 or 2 mm radius particles loaded with 10 µM sfGFP-Car9 were imaged at the indicated times after Arginine addition using confocal fluorescence microscopy and an excitation wavelength of 488 nm. All images were acquired with the same gain but particle orientation was not maintained.

of a typical radial diffusion process. Nevertheless, discrete regions of confined brightness could be detected (e.g., near the edges of the 2 mm particle at t = 6h), suggesting that the release of sfGFP-Car9 is non-ideal and affected by local pore structure.

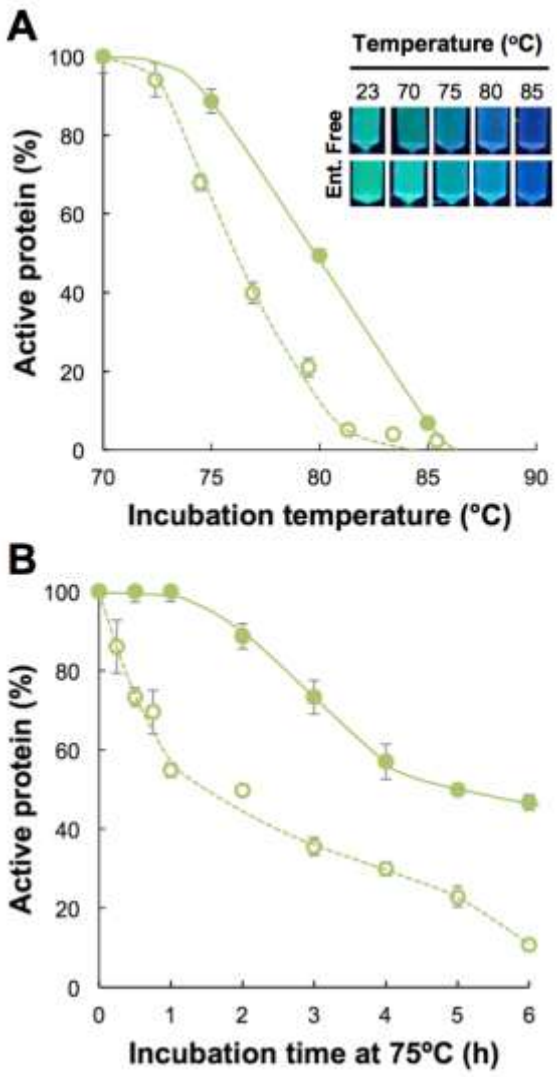

Figure 6. Sol-gel entrapment increases sfGFP-Car9 thermostability. (A) Free sfGFP-Car9 (10 µM, open symbols) or 2 mm radius particles synthesized with 10 µM of the same protein were incubated for 2h at the indicated temperatures. The entrapped proteins were released by incubation with 1M Arginine for 24h. The amount of active protein was calculated assuming that 100% activity corresponds to 65% release (see Fig. 4). (B) As in panel A except that free protein and particles were incubated at 75°C for the indicated times.

Enhanced thermostability by sol-gel network. Proteins entrapped in sol-gels often exhibit enhanced stability due to confinement effects. To determine if this would be the case with our system, we exposed 2 mm radius particles synthesized in the presence of sfGFP-Car9 to temperatures ranging from 70 to 85°C for 2h or to increasing periods of time at 75°C. Compared to free sfGFP-Car9, entrapment increased the mid-point unfolding temperature by 4°C (Figure 6A) and increased the time needed to experience a 50% decrease in initial fluorescence at 75°C from 2h to 5h (Figure 6B). Although sfGFP denaturation is a fairly complicated two-step process, [29, 30] the data presented in Figure 6 clearly demonstrate that Car9-mediated sequestration within a porous silica network increases sfGFP-Car9 thermostability.

Discontinuous protein release. To determine if sfGFP-Car9 release could be modulated by discontinuous addition of Arginine, we prepared 2 mm radius particles in the presence of 10 µM sfGFP-Car9 and initiated protein release with 1M Arginine as above. In these experiments, however, the buffer was exchanged for Tris-HCl, pH 8.5 after 1.5 or 2h of incubation. Figure 7 shows that this operation rapidly arrested sfGFP-Car9 release and that there was little evolution of the supernatant fluorescence while the particles were maintained in this buffer. Transfer to Arginine solutions after 2 or 3h restarted the release process with initial kinetics that appeared proportional to the concentration gradient. Similar amount of sfGFP-Car9 was released after 24h in all cases. This simple buffer exchange strategy should prove valuable to dynamically control the release of entrapped protein cargos.

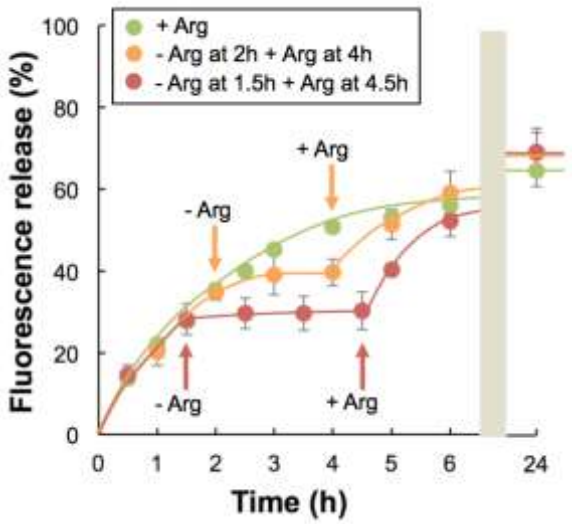

Figure 7. Dynamic control of sfGFP-Car9 release. Spherical (r = 2 mm) particles synthesized in the presence of 10 µM sfGFP-Car9 were incubated in 20 mM Tris-HCl, pH 8.5 supplemented with 1M Arginine for 1.5 or 2h before being transferred to 20 mM Tris-HCl, pH 8.5 alone. After 2 or 3h, the particles were once again taken into buffer containing 1M Arginine. The control dataset (+ Arg) is identical to that of Fig. 4).

Release of multiple entrapped proteins. An ability to chemically control the release of multiple proteins from sol-gel matrices is desirable for certain applications (e.g., catalytic cascades). To explore this possibility, sfGFP-Car9 and mCherry-Car9 (a fusion protein between the red fluorescent mCherry and the Car9 tag)[11] were mixed at a concentration of 5 µM in a solution of pre-hydrolyzed TMOS and 2 mm radius spheres were manufactured in silicone oil as above. The particles exhibited a uniform yellow-orange color when illuminated at 365 nm, suggesting that the two proteins were homogeneously distributed within the sol-gel matrices

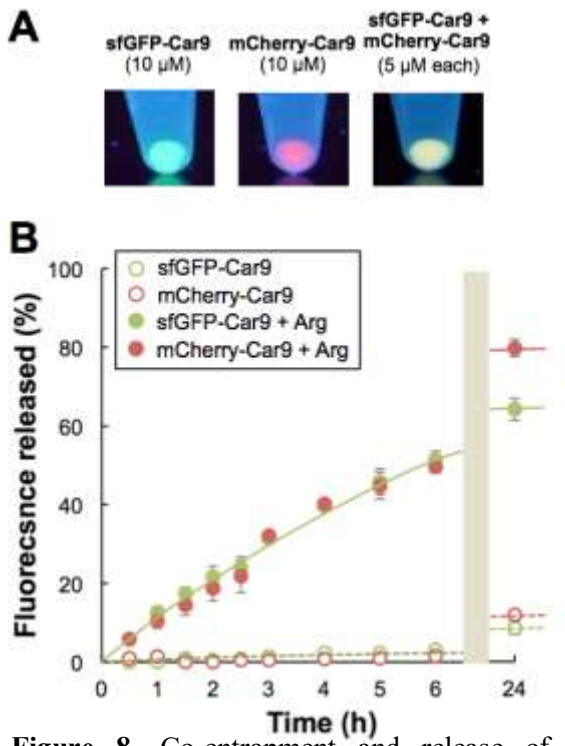

Figure 8. Co-entrapment and release of sfGFP-Car9 and mCherry-Car9 (A) Spherical (r = 2 mm) particles were synthesized in the presence of 10 μM sfGFP-Car9, 10 μM or 5 μM of each protein. Particle were photographed under UV illumination. (B) A single r = 2 mm particle was transferred to 20 mM Tris-HCl, pH 8.5 buffer lacking (open symbols) or containing 1 M Arginine (closed symbols). The fluorescence in the supernatants was assayed at the indicated time points with excitation at 475 nm (sfGFP-Car9) or 585 nm (mCherry-Car9). Error bars correspond to triplicate independent experiments. A value of 100% corresponds to the fluorescence of a 5 μM solution of sfGFP-Car9 or mCherry-Car9.

(Figure 8A). Consistent with what was observed with sfGFP-Car9 alone (Figure 4), about 12% of the entrapped mCherry-Car9 (and of the co-immobilized sfGFP-Car9) escaped the particles after 24h of incubation in pH 8.5 buffer (Figure 8B, open symbols). However, at the protein load used in these experiments, little sfGFP-Car9 or mCherry-Car9 made its way into the supernatant in the first 6h of incubation. When the particles were exposed to 1M Arginine, both proteins were liberated at nearly identical rates. Protein release was a linear function of time for the first 6h and the initial rates were 50% lower than those observed when 10 μM sfGFP-Car9 was entrapped in 2 mm radius particles (Compare filled circles in Figures 4 and 8). We conclude that multiple Car9-tagged proteins can be homogenously incorporated within silica sol-gels and concomitantly released by Arginine treatment. The fact sfGFP-Car9 and mCherry-Car9 are both β-barrel proteins of similar sizes (28.6 vs. 30.7-kDa) and pIs (6.8 vs. 6.6) explain the very similar release kinetics.

Conclusion

Bioencapsulation has been widely applied from therapy and diagnostics to drug delivery and production.[8] Silica sol-gel provides transparent and robust three-dimensional network for preservation of active biological species. With achievement of bio-immobilization, controllable release of entrapped molecules has continuously drawn attention for medical applications, especially in drug delivery. Typical methods include cleavable bonds between the targeted species and the support, and functionalized coatings on the surface which can be altered. Here we present a study on chemically-addressable release of protein entrapped in silica sol-gel by introducing a silica-binding peptide attached to the protein. The basic and hydrophilic dodecapeptide Car9 isolated by flagella display with two Arginine residues has affinity to silica, and the interaction can be disrupted by Arginine.[14] The unique characterizations allow us to study the controllable release of protein entrapped in silica sol-gels under various conditions. First, the Car9 tag enables long-term protein storage with chemically-tunable release. Arginine supplementation at higher pH and smaller particle size accelerate the kinetics and increase the amount of protein released. Second, the release can be paused temporarily and later be resumed by discontinuous addition of Arginine. In addition, Car9 mediated sequestration within silica sol-gel matrices can be partly shielded from heat denaturation and the protein thermostability is enhanced. Last, multiple Car9-tagged protein can be co-entrapped in silica sol-gel matrices and released concomitantly. The release profile is studied and compared with general spherical diffusion model to yield effective diffusion coefficients. Taking fluorescent protein as model protein, the fluorescence serves as an important indicator to quantify the amount and activity of protein presented in the system, with qualitative support by UV-Vis and confocal microscopy. In addition, pore analysis by BJH method and morphological characterization on the surface by SEM microscopy provide direct examination on the silica sol-gel matrices.

Although we have immobilized β-barrel shaped fluorescent protein, we propose that the characterizations and properties discussed above can be analogized to other enzymes or macro-proteins once with Car9 solid-binding peptide attached. This study demonstrates chemically-addressable protein entrapment in silica sol-gel matrices, providing an alternative approach for controllable release of bioencapsulation.

Experimental Procedures

Protein Purification. *E. coli* BL2(DE3) harboring plasmid pET-24a(+)-sfGFP pET-24a(+)-sfGFP-Car9 or pET-24a(+)-mCherry-Car9, which encode sfGFP, sfGFP-Car9 or mCherry-Car9 under T7 transcriptional control, respectively,[11] were grown overnight at 37 °C in 25 mL of LB medium supplemented with 50 μg/mL of kanamycin. Seed cultures were used to inoculate 500 mL of supplemented LB, cells were grown at 37 °C to A_{600} ~ 0.5 and protein expression was induced by addition of 1mM isopropyl β-*D*-thiogalactopyranoside (IPTG). Cells were harvested 5 h post-induction by centrifugation at 4,000*g* for 10 min. The pellet was resuspended in 35 mL of 20 mM Tris-HCl, pH 7.5 (Buffer A), supplemented with 2 mM EDTA and disrupted by 6 rounds of sonication for 3 min on a Branson sonifier operated at 30 % duty cycle. Lysates were centrifuged at 10,000*g* for 10 min and incubated at 70°C (sfGFP and sfGFP-Car9) or 50°C (mCherry-Car9) for 10 min to promote the aggregation of thermolabile host proteins. Insoluble material was removed by centrifugation as above. Car9-tagged proteins were purified by rapid silica-affinity chromatography essentially as described.[13] Briefly, 5g of silica gel (35-60 mesh, 15 nm pore size, Sigma-Aldrich) equilibrated in Buffer A was packed in a 1 cm inner diameter chromatography column (GE Healthcare). Lysates (35 mL) were loaded by aspiration and the column was washed with 30 mL of the same buffer. The protein was eluted with 45 mL of Buffer A supplemented with 1 M arginine. Untagged sfGFP was purified by FPLC on a Whatman DE52 anion exchange cellulose column (GE Healthcare) equilibrated in 20 mM Tris-HCl, pH 8.0 and developed at 1 mL/min. The protein was eluted in 20 mM Tris-HCl, pH 8 supplemented with 1 M NaCl using a 45 mL gradient. Purified proteins were dialyzed against 3L of Buffer A using 10-kDa molecular weight cutoff SnakeSkin tubing (Thermo Scientific) and subjected to 3 buffer changes to ensure complete arginine removal. Proteins were

concentrated using 10-kDa microconcentrators (Merck) and stored at -20 °C at a 25 µM final concentration (0.66 mg/mL for sfGFP, 0.71 mg/mL for sfGFP-Car9 and 0.76 mg/mL for mCherry-Car9).

Protein Entrapment in Silica Sol-Gels. Proteins were entrapped in silica sol-gels formed by condensation of silicic acid prepared by acid hydrolysis of tetramethyl orthosilicate (TMOS)[18] with the following modifications. A 15 µL aliquot of TMOS (99% purity, 6.6 M; Acros, NJ) was mixed with 40 µL of ddH_2O and 5 µL of 20 mM HCl (20 mM) and the solution was subjected to 5 cycles of 20 s vortexing followed by 40 s rest periods. Proteins were mixed with the solution at a final concentration of 10 µM and final volume of 100 µL by pipetting.

Hemispheroidal sol-gels particles were produced by depositing 30 µL of the resulting solution on 3.2 mm diameters polycarbonate filters bounded by a hydrophobic ring and arranged in 96-well format (ChemoTx system, Neuro Probe, Gaithersburg, MD). The filter plates were placed in a chamber sealed with parafilm and sol-gel formation was allowed to proceed for 4h. The particles were removed with a spatula for long term storage in 1 mL of Buffer A at room temperature.

Spheroidal particles were produced by releasing 4.2 µL, 14.1µL or 33.5 µL of protein/silicic acid solution from a pipette tip and into 400 µL of silicone oil (poly dimethylsiloxane, CAS:63148-62-9, Pitney Bowes). This led to the formation of particles ~1, 1.5 or 2 mm in radius, respectively. After 4 h incubation at room temperature, the oil was removed and the particles were washed three times with Buffer A supplemented with 0.02% (w/v) Tween20) in order to remove residual silicone oil.[23] Samples were stored in 1 mL of Buffer A.

Fluorescence Measurements. To monitor protein release from hemispheroidal sol-gels, samples consisting of a single sfGFP-Car9 or sfGFP particle in 1 mL of Buffer A supplemented

or not with 1 M Arginine were prepared in triplicate. Tubes were mounted on a Dynabeads rotary sample mixer (Invitrogen) operated at room temperature and 60 rpm. Triplicate samples (100 µL) were harvested at the indicated time points, transferred to a black 96-wells microplate (Greiner) and the fluorescence was measured at 510 nm on a SpectraMax M5 microplate reader (Molecular Devices) with excitation at 475 nm and a cut-off wavelength of 495 nm. All samples were returned to the original tube after measurements with negligible sample loss. Similar experiments were conducted in 20 mM Tris-HCl, pH 8.5 to delineate the influence of pH. Measurements of protein release from spheroidal sol-gels were performed as above in 20 mM Tris-HCl pH 8.5 except that 4 particles (r = 1mm), 2 particles (r = 1.5 mm) or a single particle (r = 2 mm) were placed in each tube to allow for easy detection of fluorescence at early time points.

For discontinuous release experiments, a 2 mm radius silica sol-gel bead loaded with sfGFP-Car9 was placed in 1 mL of 20 mM Tris-HCl, pH 8.5 supplemented with 1M Arginine in triplicate tubes. The fluorescence of the samples was monitored as above except that after 1.5 or 2h, the supernatant was harvested and reserved. Particles were washed 3 times with 20 mM Tris-HCl, pH 8.5, placed in 1 mL of same buffer and returned to the shaker. The fluorescence of the supernatants and that of the reserved samples were quantified at 1h intervals. These values were added to produce the plotted data. After 2 or 3h of incubation in Tris-HCl solutions, beads were retaken in their original arginine-containing buffer and supernatant fluorescence was monitored as above.

For the experiments of Fig. 8, sfGFP-Car9 and mCherry-Car9 at 5 µM each were entrapped within 2 mm radius particles as above. Triplicate tubes containing a single bead were supplemented with 1 mL of 20 mM Tris-HCl, pH 8.5 supplemented or not with 1M arginine and protein release was quantified 5 as above for sfGFP-Car9 and using an excitation wavelength of

585 nm, emission wavelength of 625 nm and a cut-off wavelength of 610 nm for mCherry-Car9. There was negligible bleed-through between fluorescence channels. All samples were photographed under 365 nm excitation using a UV transilluminator.

Thermostability measurements. Triplicate tubes containing 1 mL of Buffer A and a single 2 mm radius silica bead loaded with 10 μM sfGFP-Car9 were incubated at 75°C for the indicated times in a heating block. At the end of each incubation step, the beads were transferred to 1 mL of 20 mM Tris-HCl, pH 8.5 supplemented with 1M arginine and incubated for 24h to achieve maximum protein release (~70% of the load). Supernatant fluorescence was measured as above and the fraction of active protein was determined by dividing these numbers by the mean fluorescence released with no heat treatment and 24h of incubation in 20 mM Tris-HCl, pH 8.5 1M arginine at room temperature. For control experiments, free sfGFP-Car9 (10 μM in 1 mL of Buffer A) was incubated at 75ºC for the indicated times. The fraction of active protein was determined by dividing the fluorescence at these time points to that of the original solution. Thermostability of entrapped sfGFP-Car9 at high temperatures was determined as above except that the incubation time was set at 2h.

General techniques: A Nikon Confocal Microscope A1 and the NIS-Elements AR Microscope Imaging Software were used for acquisition of confocal images with laser excitation at 488 nm.

sfGFP-Car9 entrapped in r=2 mm spherical sol-gels were taken for pore analysis. Particles were removed from Tris-HCl, pH 7.5, replaced with 2 mL anhydrous ethanol (Sigma), and incubated for five days with three times of solvent exchange. Beads were then loaded on the critical point dryer (Quorum E3100), filled with liquid CO_2 and incubated for two days. The temperature was held at 10°C with a water circulator. Periodically, the vessel was purged with

ethanol and refilled with fresh liquid CO_2 simultaneously. Then the circulator was used to raise the temperature to 38°C, which was above the critical point temperature of 31°C to ensure all fluid turned supercritical. The vessel was vented slowly to prevent re-condensation of CO_2 caused by rapid cooling. After venting to atmosphere, the vessel was cooled naturally to room temperature before removing the dried particles.

Dried particles were heated in vacuum to 160°C for 12 hours to remove any adsorbed moistures. A pore analyzer (Quantachrome NOVA 2200e) was used to collect the nitrogen isotherm at 77 K. Pore size distribution was obtained by Barrett-Joyner-Halenda (BJH) method. The necessary calculations were performed by the instrument software.

Scanning electron microscopy (SEM) was used to determine the morphology of the particles. Samples were dried as previously described and placed on a piece of carbon tape attached to an aluminum stub. The samples were sputter coated with a gold/palladium coat for 60 seconds (~10 nm thick) and imaged on a FEI XL830 Dual Beam FIB/SEM.

Supplementary Data

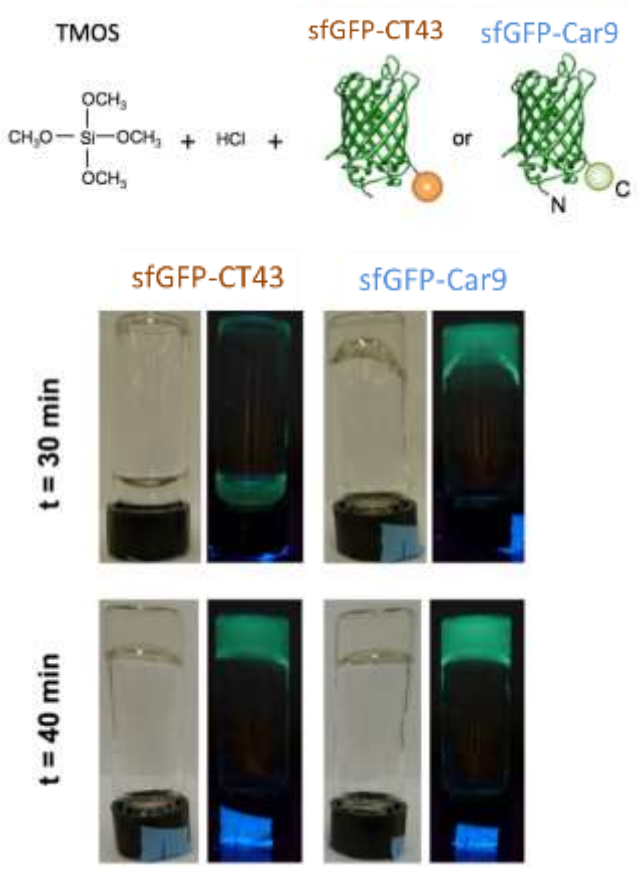

Figure S1. Entrapment of sfGFP-CT43 and sfGFP-Car9 within silica sol-gels. The ability of sfGFP-Car9 to drive sol-gel formation was demonstrated by inversion experiments at the indicated time points.

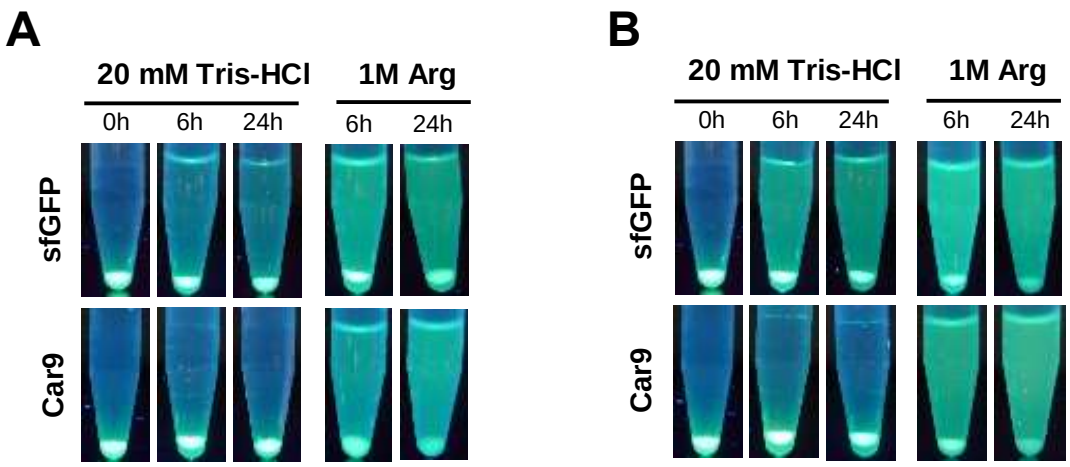

Figure S2. Effect of pH and Arginine on the release of sfGFP and sfGFP-Car9 from hemispheroidal sol-gel particles. sfGFP or sfGFP-Car9 (10 µM) entrapped in hemispheroidal silica particles were incubated at room temperature with shaking in 1 mL of 20 mM Tris-HCl buffered at pH 7.5. (A) Appearance of particles and supernatants under UV illumination at 365 nm following 0, 6 and 24h incubation in Tris-HCl or Arginine-containing solutions at pH 7.5. (B) Appearance of particles and supernatants under UV illumination at 365 nm following 0, 6 and 24h incubation in Tris-HCl or Arginine-containing solutions at pH 8.5.

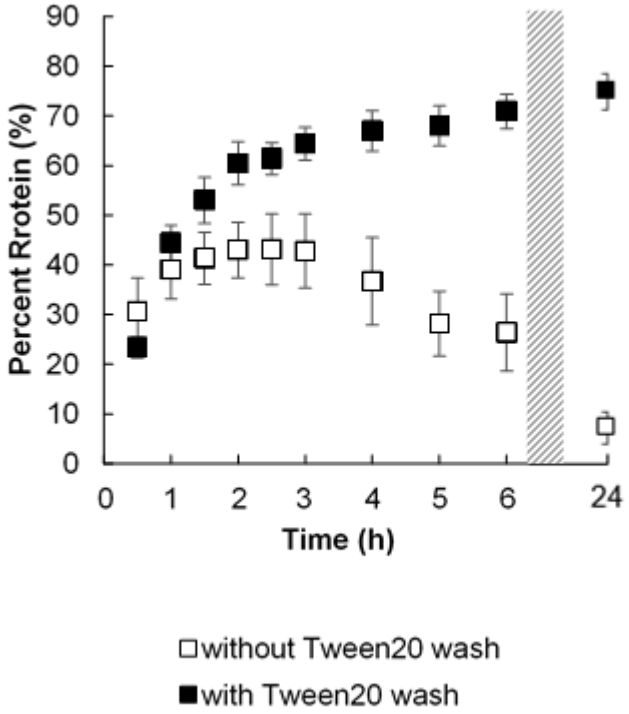

Figure S3. Influence of detergent Tween 20 in the wash buffer on the sfGFP-Car9 unfolding event when spherical particles were produced in silicone oil. Protein (10 μM) was entrapped within 1 mm radius particles as described in Experimental Procedures. Four 1 mm radius spherical particles were transferred to 20 mM Tris-HCl supplemented with 1M Arginine at pH 8.5 lacking (open symbols) or with detergent Tween 20 (closed symbols) in the wash buffer. The fluorescence in the supernatants was assayed at the indicated time points. Error bars correspond to triplicate independent experiments. A value of 100% corresponds to the fluorescence of a 10 μM solution of sfGFP-Car9.

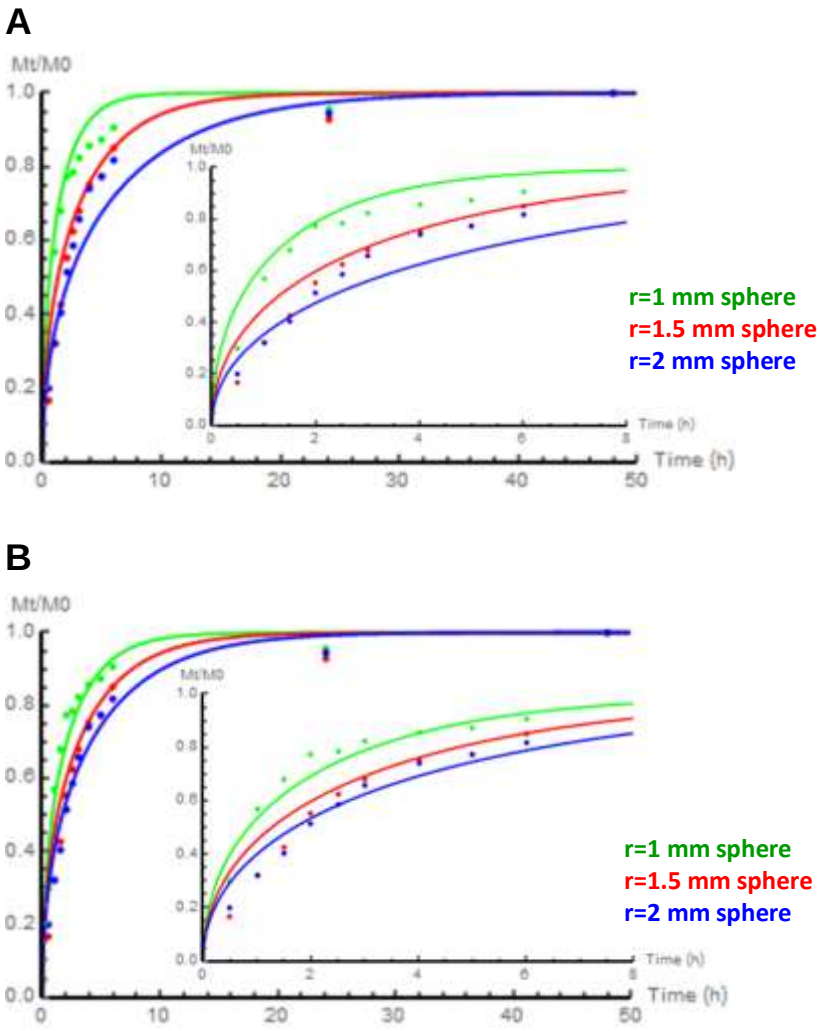

Figure S4. Fitting experimental data of sfGFP-Car9 (10 μM) entrapped in different sizes of spherical silica particles (r = 1 mm, 1.5 mm, 2 mm) and incubated in 20 mM Tris-HCl supplemented with 1M Arginine at pH 8.5 at room temperature with Ritger-Peppas model[26] (with admittedly unmet assumptions). 48h release data was assumed for calculating M_0. (A) Fitting the release profile for all three sizes of particles with constant diffusion coefficient of 1.5 x 10^{-7} cm^2/s. (B) Fitting the release profile for three sizes of particles with effective diffusion coefficients: 1 x 10^{-7} cm^2/s for r = 1 mm radius spherical particles; 1.5 x 10^{-7} cm^2/s for 1.5 mm radius spherical particles, and 2 x 10^{-7} cm^2/s for 2 mm spherical particles.

Reference

(1) Vallet-Regi, M., Ramila, A., del Real, R. P., and Perez-Pariente, J. (2001) A new property of MCM-41: Drug delivery system. *Chem. Mater. 13*, 308-311.

(2) Manzano, M., and Vallet-Regi, M. (2010) New developments in ordered mesoporous materials for drug delivery. *J. Mater. Chem. 20*, 5593-5604.

(3) Wang, Y., Zhao, Q., Han, N., Bai, L., Li, J., Liu, J., Che, E., Hu, L., Zhang, Q., Jiang, T., and Wang, S. (2015) Mesoporous silica nanoparticles in drug delivery and biomedical applications. *Nanomedicine 11*, 313-27.

(4) Kandimalla,V. B., Tripathi, V. S., Ju, H. (2006) Immobilization of Biomolecules in Sol–Gels: Biological and Analytical Applications. *Critical Reviews in Analytical Chemistry. 36, 2*, 73-106.

(5) Bhatia, R. B., Brinker, C. J. (2000) Aqueous Sol−Gel Process for Protein Encapsulation. *Chem. Mater., 12 (8)*, 2434–2441.

(6) Buthe, A. (2011) Entrapment of enzymes in nanoporous sol-gels. *Methods Mol. Biol. 743*, 223-37.

(7) Jin, W., and Brennan, J. D. (2002) Properties and applications of proteins encapsulated within sol-gel derived materials. *Anal. Chim. Acta 461*, 1-36.

(8) Wang, X., Ahmed, N. B., Alvarez, G. S., Tuttolomondo, M. V., Helary, C., Desimone, M. F., and Coradin, T. (2015) Sol-gel encapsulation of biomolecules and cells for medicinal applications. *Curr. Top. Med. Chem. 15*, 223-44.

(9) Slowing, I. I., Trewyn, B. G., Giri, S., and Lin, V. S. Y. (2007) Mesoporous silica nanoparticles for drug delivery and biosensing applications. *Adv. Funct. Mater. 17*, 1225-1236.

(10) Mamaeva, V., Sahlgren, C., and Linden, M. (2013) Mesoporous silica nanoparticles in medicine--recent advances. *Adv Drug Deliv Rev 65*, 689-702.

(11) Lai, C. Y., Trewyn, B. G., Jeftinija, D. M., Jeftinija, K., Xu, S., Jeftinija, S., and Lin, V. S. (2003) A mesoporous silica nanosphere-based carrier system with chemically removable CdS nanoparticle caps for stimuli-responsive controlled release of neurotransmitters and drug molecules. *J. Am. Chem. Soc. 125*, 4451-9.

(12) Liu, R., Zhang, Y., Zhao, X., Agarwal, A., Mueller, L. J., and Feng, P. (2010) pH-responsive nanogated ensemble based on gold-capped mesoporous silica through an acid-labile acetal linker. *J. Am. Chem. Soc. 132*, 1500-1.

(13) Coyle, B. L., and Baneyx, F. (2014) A cleavable silica-binding affinity tag for rapid and inexpensive protein purification. *Biotechnol. Bioeng. 111*, 2019-26.

(14) Coyle, B. L., Rolandi, M., and Baneyx, F. (2013) Carbon-binding designer proteins that discriminate between sp2- and sp3-hybridized carbon surfaces. *Langmuir 29*, 4839-4846.

(15) Coyle, B. L., and Baneyx, F. (2016) Direct and reversible immobilization and microcontact printing of functional proteins on glass using a genetically appended silica-binding tag. *Chem. Commun. (Camb.) 52*, 7001-4.

(16) Kroger, N., Deutzmann, R., and Sumper, M. (1999) Polycationic peptides from diatom biosilica that direct silica nanosphere formation. *Science 286*, 1129-1132.

(17) Naik, R. R., Whitlock, P. W., Rodriguez, F., Brott, L. L., Glawe, D. D., Clarson, S. J., and Stone, M. O. (2003) Controlled formation of biosilica structures in vitro. *Chem. Commun. (Camb.)*, 238-9.

(18) Luckarift, H. R., Spain, J. C., Naik, R. R., and Stone, M. O. (2004) Enzyme immobilization in a biomimetic silica support. *Nat. Biotechnol. 22*, 211-3.

(19) Luckarift, H. R., Dickerson, M. B., Sandhage, K. H., and Spain, J. C. (2006) Rapid, room-temperature synthesis of antibacterial bionanocomposites of lysozyme with amorphous silica or titania. *Small 2*, 640-3.

(20) Pedelacq, J. D., Cabantous, S., Tran, T., Terwilliger, T. C., and Waldo, G. S. (2006) Engineering and characterization of a superfolder green fluorescent protein. *Nat. Biotechnol. 24*, 79-88.

(21) Zhou, W., Schwartz, D. T., and Baneyx, F. (2010) Single pot biofabrication of zinc sulfide immuno-quantum dots. *J. Am. Chem. Soc. 132*, 4731-4738.

(22) Davis, P. J., Brinker, C. J., and Smith, D. M. (1992) Pore Structure Evolution in Silica-Gel during Aging Drying .1. Temporal and Thermal Aging. *J. Non-Cryst. Solids 142*, 189-196.

(23) Davis, P. J., Brinker, C. J., Smith, D. M., and Assink, R. A. (1992) Pore Structure Evolution in Silica-Gel during Aging Drying .2. Effect of Pore Fluids. *J. Non-Cryst. Solids 142*, 197-207.

(24) Santos, E. M., Radin, S., and Ducheyne, P. (1999) Sol-gel derived carrier for the controlled release of proteins. *Biomaterials 20*, 1695-700.

(25) Dixit, N., Maloney, K. M., and Kalonia, D. S. (2012) The effect of Tween® 20 on silicone oil-fusion protein interactions. *Int. J. Pharm. 429*, 158-67.

(26) Ritger, P. L., and Peppas, N. A. (1987) A simple equation for description of solute release I. Fickian and non-Fickian release from non-swellable devices in the form of slabs, spheres, cylinders or discs. *J. Control. Rel. 5*, 23-36.

(27) Hungerford, G., Rei, A., Ferreira, M. I., Suhling, K., and Tregidgo, C. (2007) Diffusion in a sol-gel-derived medium with a view toward biosensor applications. *J. Phys. Chem. B 111*, 3558-62.

(28) Dayel, M. J., Hom, E. F., and Verkman, A. S. (1999) Diffusion of green fluorescent protein in the aqueous-phase lumen of endoplasmic reticulum. *Biophys. J. 76*, 2843-51.

(29) Campanini, B., Bologna, S., Cannone, F., Chirico, G., Mozzarelli, A., and Bettati, S. (2005) Unfolding of Green Fluorescent Protein mut2 in wet nanoporous silica gels. *Protein Sci. 14*, 1125-33.

(30) Hsu, S. T., Blaser, G., and Jackson, S. E. (2009) The folding, stability and conformational dynamics of beta-barrel fluorescent proteins. *Chem. Soc. Rev. 38*, 2951-65.